

Experimental study on fluid-structure interaction of a fish-like model at high angle of attack

Xi He¹, Jinjun Wang^{1*}

¹Beihang University, Key Laboratory of Fluid Mechanics (Ministry of Education), Beijing, China

*jjwang@buaa.edu.cn

Abstract

A particle image velocimetry (PIV) experiment is carried out to investigate the fluid-structure interaction between a fish-like model and an incoming flow at Reynolds number of 3.57×10^4 (based on the length of model). The model is composed of a rigid NACA0020 airfoil and a flexible extended trailing edge plate. The kinematic characteristics of the flexible trailing edge plate is firstly analyzed. While interacting with the fluid, the flexible plate will perform strong periodic vibration, and present an undulatory mode. The flow field is also captured in this study. It is found that the vibration of the flexible plate causes the generation and shedding of trailing edge vortex. Compared with the rigid trailing edge plate, this study further shows that the flexible one can greatly reduce the velocity deficit in the wake and suppress the post-stall separation at high angle of attack.

1 Introduction

Swimming performance of fish has always been a hot issue in the field of fluid mechanics. In the early studies of Lighthill (1970), Wu (1971), Katz and Weihs (1978), the flexible bodies of aquatic animals are found to have excellent hydrodynamic characteristics. The undulatory propulsion mode of such aquatic animals tends to improve speed and hydrodynamic efficiency. Based on the rigidity of fish bodies, the structure of fish can be divided into four categories: anguilliform, subcarangiform, carangiform and thunniform (Lindsey (1978)). Accordingly, the movement of most fish can be simplified as the fluid-structure interaction of a rigid forebody and a flexible trailing edge plate in an incoming flow.

Numerous studies aimed to find out the mechanism of fluid-structure interaction of flexible plates or flags have been conducted. It was indicated in the soap film tunnel experiment by Zhang (2000) that the flexible flag performs three different modes with the flag length and flow velocity increasing: stretched straight mode, coherent flapping mode and chaotic flapping mode. The corresponding amplitude and frequency of each mode are also variable. Eloy et al. (2007, 2008) analyzed the flutter instability of cantilevered flexible plates theoretically and experimentally. They pointed out that the instability of flexible plates or flags is due to the competition between destabilizing pressure forces and stabilizing bending stiffness. Further investigations of Connell and Yue (2007), Shelley and Zhang (2011) showed that the flutter modes of flag is related to Reynolds number (Re), the mass ratio of flag to fluid and the flag rigidity. Chaotic flapping mode is easier to occur for the flag with higher Re , larger mass ratio and less rigidity. However, a majority of these works rarely considered the flow structures. The fluid-structure interaction of flexible plates is common phenomena in nature and engineering. Watanabe (2002) indicated that the increase of paper printing speed will cause paper flutter and rupture, thereby reducing production efficiency. Allen and Smits (2001) placed a piezoelectric flexible plate in the wake of a bluff body, the Karman vortex street of which can induce deformation and vibration of the plate, thus generating electricity. Moreover, such fluid-structure interaction phenomenon also has an effective application in stall control. Pantula (2008) suggested controlling post-stall separation of NACA0012 airfoil by attaching flexible fin on the upper surface of the airfoil. Liu et al (2009, 2010) supplemented the work of Pantula (2008) experimentally and indicated that

drag reduction and oscillation suppression particularly for the natural low frequency oscillation in deep stall are achieved by using a flexible fin attached at a suitable location on the NACA0012 airfoil. Liu et al (2007) discovered that attaching a static extended trailing edge behind the NACA0012 airfoil can achieve lift enhancement at a small drag penalty. They prospected the great potential of flexible extended trailing edge to improve the cruise flight efficiency and control separation.

Inspired by Liu et al. (2007, 2009), this paper conducts a PIV experiment to study a fish-like model consisting of a rigid NACA0020 airfoil and a flexible extended trailing edge plate at high angle of attack. The kinematic characteristics of the plate as well as the flow field are both analyzed to explore the interaction of the model and surrounding fluid. The full text is divided into following parts: introduction, experimental method, kinematic characteristics of the flexible plate, flow field and conclusion.

2 Experimental method

The present experiment is carried out in the low-speed, self-circulating water tunnel at Beihang University. The schematic diagram of the PIV experimental set-up is illustrated in Figure 1. The test section of the water tunnel is 3m long with a cross-section size of 0.6m (width) \times 0.7m (height). The freestream velocity (U_∞) is 0.30m/s and the turbulent intensity (σ) is less than 1% in this experiment. As shown in Figure 2, the fish-like model is composed of an aluminum NACA0020 airfoil and a flexible extended trailing edge plate. With the chord length of the airfoil (C) to be 60mm and the size of the flexible plate to be 80mm (length (L)) \times 80mm (width) \times 0.1mm (thickness), the corresponding characteristic length ($D=C+L$) is 140mm, resulting in the Reynolds number based on D (Re_D) being equal to 3.57×10^4 . The material of this flexible plate is polycarbonate with modulus of elasticity and Poisson ratio of 780MPa and 0.4, respectively. In order to facilitate the connection, a slot is cut along the chord in the rear of the airfoil into which the flexible plate can be inserted. As a result, the trailing edge plate can be approximated to a cantilever plate with one end fixed and the other end free. The angle between the airfoil chord and freestream (α) is 30° , which belongs to the post-stall angle of attack. For comparison, a rigid aluminum trailing edge plate with the same size is also adopted to be a reference.

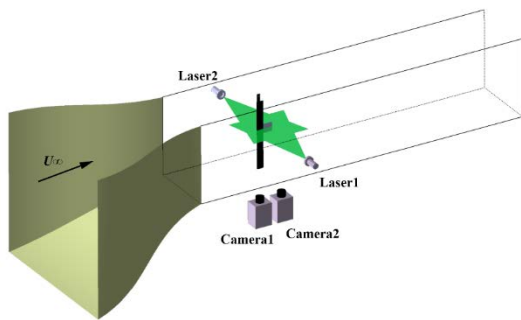


Figure 1: The schematic diagram of the PIV experiment.

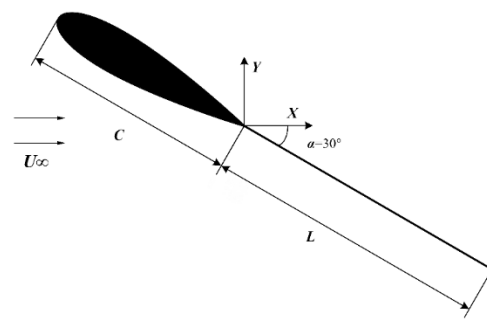


Figure 2: The fish-like model.

The high-speed laser with the frequency up to 1 kHz is used in the PIV experiment as a light source. In order to get the required flow field, two parallel laser sheets of approximately 1.0mm thickness are irradiated from both sides of the model to illuminate the measured area. Hollow glass beads with diameter of 5~10 μ m are employed as tracer particles and the density is 1.05g/mm³, which is close to water density. Two synchronous high-speed CMOS cameras mounted along streamwise direction are employed in the present study to capture the motion of flexible trailing edge and flow structures simultaneously. The sampling speed is set

to be 400Hz due to the freestream velocity. The resolution of each camera is 2048×2048 pixels and the field of view (FOV) is about $170\text{mm} \times 170\text{mm}$, resulting in the magnification being 0.083mm/pixel . The raw images are processed based on the multiple iterative Lucas-Kanade algorithm (MILK) (Champagnat et al. (2011)) to obtain original velocity field. The interrogation window size is set to be 32×32 pixels with 75% overlap rate and the number of velocity vectors are 256×256 .

3 Results

3.1 Kinematic characteristics of the flexible trailing edge plate

In this paper, the flexible trailing edge plate attached to the airfoil will vibrate while interacting with the fluid. The vibration frequency of the plate (f_{pl}) can be attained by conducting the fast Fourier transform (FFT) on the vertical movement at the end of the plate. The spectrum of plate vibration is shown in Figure 3 and the power spectrum density is normalized by its maximum value. It is obvious that the vibration of this flexible trailing edge plate is a strong periodic motion with a frequency of 1.54Hz.

To intuitively reflect the motion of the flexible plate, the vibration patterns in one period is presented in phase (Φ) sequences in Figure 4. The phase $\Phi=0^\circ$ is defined corresponding to the time when the end of the plate vibrates to the highest vertical position. It can be found that the end of the plate reach the lowest position at around $\Phi=180^\circ$. The vibration pattern at $\Phi=90^\circ$ expressed in red solid line presents an undulatory mode with several inflection points on the curve, which reflects the complexity of the flow field.

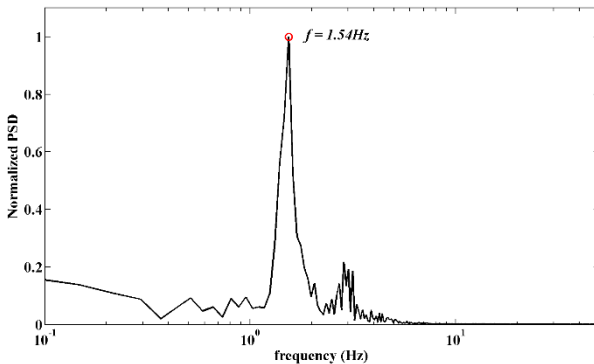


Figure 3: Frequency spectrum of the flexible trailing edge plate.

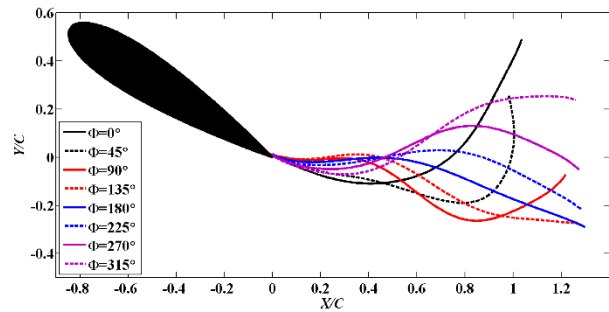


Figure 4: Vibration patterns in one period.

3.2 Flow field

The phase-averaged flow field is also presented in phase sequences in Figure 5. The X and Y positions are normalized by C . There always exists a separation region at the leeward airfoil surface. At $\Phi=0^\circ$ when the end of the flexible plate is at the highest vertical position, there is a counter-clockwise vortex (hereinafter referred to as the trailing edge vortex) near the end of plate. Subsequently, the flexible plate moves towards the negative direction of Y , resulting in the extrusion of trailing edge vortex. When Φ reaches to 90° , the trailing edge vortex goes above the flexible plate. As Φ continues to increase, the trailing edge vortex gradually sheds from the plate and then dissipates downstream. The trailing edge vortex is no longer seen from the streamline at $\Phi=180^\circ$ when the end of the plate reaches the lowest vertical position. Then the flexible plate begins to move towards the positive direction of Y , and the trailing edge vortex appears beneath the plate at $\Phi=315^\circ$. For comparison, the time-averaged flow field of rigid trailing edge plate case is shown

in Figure 6. Compared with the flexible case, the separation region is much larger, which means the existence of flexible trailing edge plate greatly suppresses the post-stall separation at high angle of attack.

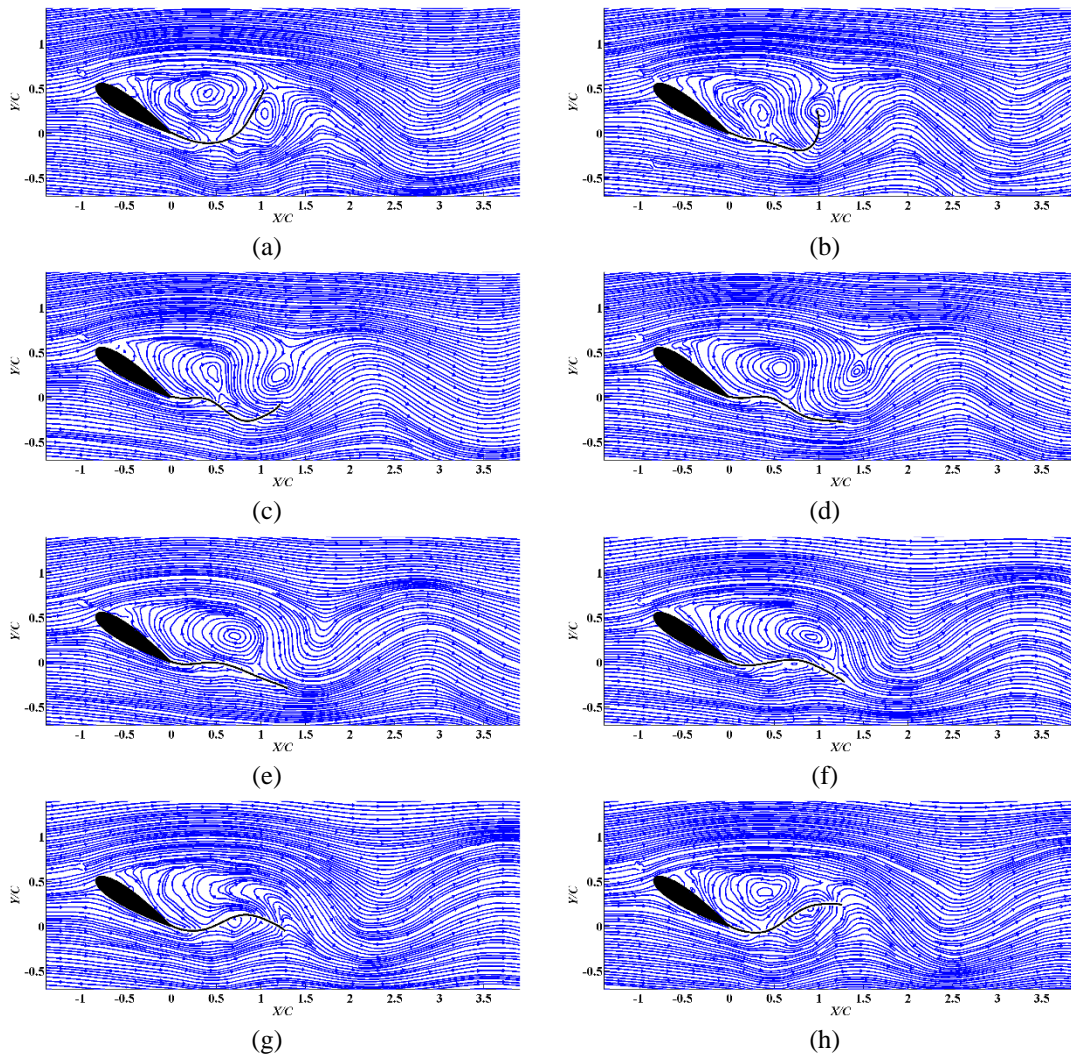


Figure 5: Phase-averaged flow field of flexible trailing edge plate case. (a) $\Phi=0^\circ$; (b) $\Phi=45^\circ$; (c) $\Phi=90^\circ$; (d) $\Phi=135^\circ$; (e) $\Phi=180^\circ$; (f) $\Phi=225^\circ$; (g) $\Phi=270^\circ$; (h) $\Phi=315^\circ$.

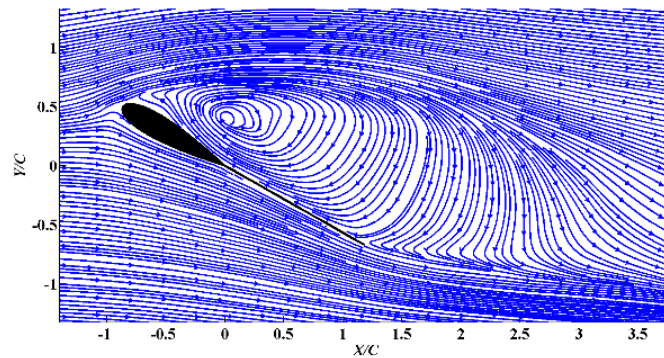


Figure 6: Time-averaged flow field of rigid trailing edge plate case.

Figure 7 presents the minimum value evolution of the time-averaged streamwise velocity (U) along the downstream direction. The time-averaged streamwise velocity distributions at the chosen four streamwise positions ($X/C=0.5, 1.5, 2.5$ and 3.5) are further shown in Figure 8. The black lines and the blue lines represent the flexible and rigid cases respectively. U is nondimensionalized by U_∞ . As shown in Figure 7, the streamwise velocities in these two cases both reach the minimum value at around $X/C=0.3$. It means that the magnitude of streamwise velocity deficit is the highest at this position. In Figure 8, the streamwise velocity deficits in these two cases both decreases gradually at these four positions. Besides, the magnitude and vertical range of velocity deficit in the flexible trailing edge case are less than those in the rigid case at each streamwise position. Specifically, both rigid and flexible cases suffer a great velocity deficit at $X/C=0.5$. The negative streamwise velocity at around $Y/C=0$ indicates that there is a recirculation zone. At $X/C=2.5$, the streamwise velocity in the flexible case restores to be positive, but the minimum streamwise velocity in the rigid case is still negative. Therefore, the flexible trailing edge plate can greatly reduce the velocity deficit in the wake, thus lead to drag reduction compared with the rigid trailing edge plate.

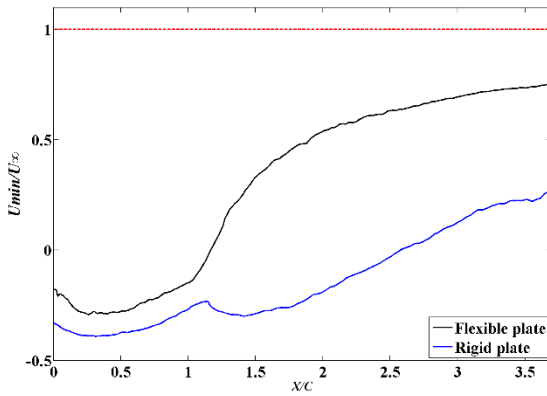


Figure 7: The minimum value evolution of streamwise velocity as flow goes downstream.

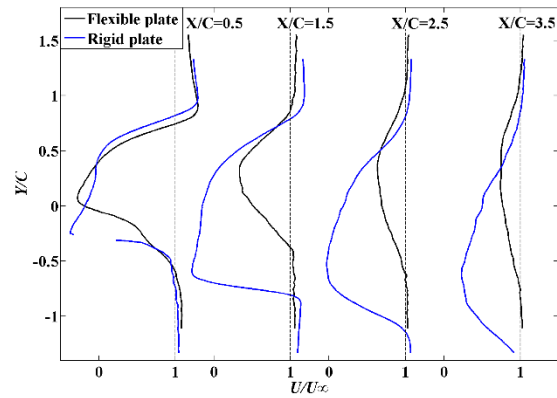


Figure 8: Time-averaged streamwise velocity distributions at different streamwise positions.

4 Conclusion

This paper discusses the fluid-structure interaction phenomenon on a fish-like model at high angle of attack. Coupled with the flow structures, the vibration of the flexible trailing edge plate in the fish-like model performs an undulatory pattern. This vibration phenomenon can help to reduce the velocity deficit in the wake and control the post-stall separation at the leeward surface of the airfoil when compared with the rigid trailing edge plate. This study makes it clear that the flexible trailing edge plate have more advantages on post-stall separation control than the rigid one.

Acknowledgements

This work was supported by the Fundamental Research Funds for the Central Universities (Nos. YWF-16-BJ-Y-06 and YWF-16-JCTD-A-05).

References

- Lighthill MJ (1970) Aquatic animal propulsion of high hydromechanical efficiency. *Journal of Fluid Mechanics* 44 (02):265-301
- Wu T (1971) Hydromechanics of swimming propulsion. Part 1. Swimming of a two-dimensional flexible plate at variable forward speeds in an inviscid fluid. *Journal of Fluid Mechanics* 46 (02):337-355
- Katz J and Weihs D (1978) Hydrodynamic propulsion by large amplitude oscillation of an airfoil with chordwise flexibility. *Journal of Fluid Mechanics* 88 (03):485-497
- Lindsey CC (1978) Form, function and locomotory habits in fish. *Fish Physiology* 7:1-100
- Zhang J, Childress S, Libchaber A and Shelley M (2000) Flexible filament in a flowing soap film as a model for one-dimensional flags in a two-dimensional wind. *Nature* 408:835-839
- Eloy C, Souilliez C and Schouveiler L (2007) Flutter of a rectangular plate. *Journal of Fluids and Structures* 23:904-919
- Eloy C, Lagrange R, Souilliez C and Schouveiler L (2008) Aeroelastic instability of cantilevered flexible plates in uniform flow. *Journal of Fluid Mechanics* 611:97-106
- Connell B and Yue D (2007) Flapping dynamics of a flag in a uniform stream. *Journal of Fluid Mechanics* 581:33-68
- Shelley MJ and Zhang J (2011) Flapping and bending bodies interacting with fluid flows. *Annual Review of Fluid Mechanics* 43 (1):449-465
- Watanabe Y, Suzuki S, Sugihara M and Sueoka Y (2002) An experimental study of paper flutter. *Journal of Fluids and Structures* 16:529-542
- Allen JJ and Smits AJ (2001) Energy harvesting eel. *Journal of Fluids and Structures* 15:629-640
- Pantula SR (2008) Modeling fluid structure interaction over a flexible fin attached to a NACA0012 airfoil. Ph.D. Thesis, Department of Mechanical and Aeronautical Engineering, Western Michigan University, Kalamazoo, MI, 2008
- Liu TS, Montefort J, Liou W, Pantula SR, Yang Y and Shams QA (2009) Post-stall flow control using a flexible fin on airfoil. 47th Aiaa Aerospace Sciences Meeting. 5-8 Jan 2009, Orlando, Florida
- Liu TS, Montefort J and Pantula SR (2010) Effects of Flexible Fin on Low-Frequency Oscillation in Poststall Flows. *AIAA Journal* 48 (6):1235-1247
- Liu TS, Montefort J, Liou W, Pantula SR and Shams QA (2007) Lift enhancement by static extended trailing edge. *Journal of Aircraft* 44 (6):1939-1947
- Champagnat F, Plyer A, Le BG, Leclaire B, Davoust S and Le Saut Y (2011) Fast and accurate PIV computation using highly parallel iterative correlation maximization. *Experiments in Fluids* 50 (4):1169-1182